Combined Supplementary Information:

Genomic activation of *PPARG* reveals a candidate therapeutic axis in bladder cancer

Jonathan T. Goldstein[1], Ashton C. Berger[1], Juliann Shih[1], Fujiko F. Duke[1], Laura Furst[1], David J. Kwiatkowski[2], Andrew D. Cherniack[1,3], Matthew Meyerson[1,3,4,5] and Craig A. Strathdee[1]

Affiliations:
[1]The Broad Institute of MIT and Harvard, Cambridge, Massachusetts, United States of America. [2]Brigham and Women's Hospital, Harvard Medical School, Boston, Massachusetts, United States of America, [3]Department of Medical Oncology, Dana-Farber Cancer Institute, Boston, Massachusetts, United States of America, [4]Center for Cancer Genome Discovery, Dana-Farber Cancer Institute, Boston, Massachusetts, United States of America. [5]Department of Pathology, Harvard Medical School, Boston, Massachusetts, United States of America,

Supplementary Methods.

Clonogenic growth assays:
Cells were plated at ~5,000 cells per well in 12-well plates in MEM alpha medium containing 10% fetal bovine serum. Compounds, as indicated, were dosed three times per week and the culture media was completely refreshed at least once per week. Cells were treated with 100 nM GW9662, 100nM T0070907, or vehicle as control. All samples were performed in triplicate. Cells were fixed with 4% paraformaldehyde and stained with crystal violet between day 7 and 19, dependent upon growth rate. For quantitative analysis, 1 ml of 10% acetic acid in water was added to each well and incubated for two hours to extract crystal violet. UV absorption of samples was measured at 570nm and test samples were normalized to the DMSO control. Relative proliferation is reported as a Percent Of DMSO Control (POC).

Quantitative PCR: RNA was harvested from cells after overnight treatment with indicated compounds using RNEasy (Qiagen, Germantown, MD). First strand cDNA was synthesized using Superscript III First Strand Synthesis (ThermoFisher Scientific, Waltham MA). Gene expression was quantified using TaqMan™ Gene Expression Master Mix (ThermoFisher Scientific, Waltham, MA) with assay probes for FABP4 (Hs01086177_m1) and GAPDH (Hs02758991_g1). Analysis was performed using QuantStudio 6 Flex Real-Time PCR (Applied Biosystems / ThermoFisher, Waltham, MA).

Supplementary Figures

Supplementary Figure 1.

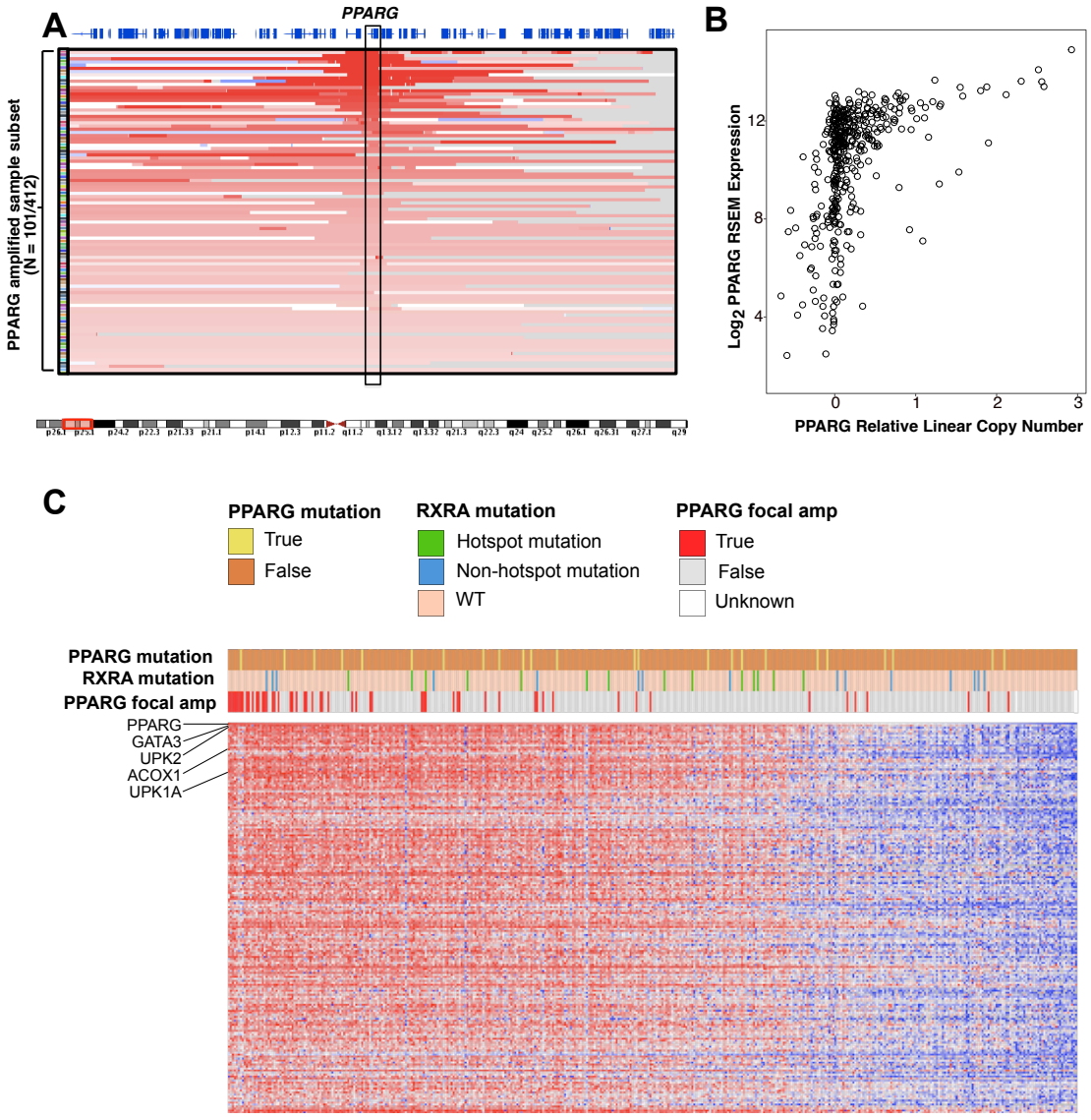

Supplementary Figure 1. Somatic alterations in PPARG and RXRA are hallmarks of luminal bladder cancer. Analysis of TCGA muscle-invasive urothelial carcinoma dataset (1) showing **A,** heatmap of gene copy number for 3p25 region sorted by PPARG copy number. Data represent the top 101 of 412 amplified samples, sorted by PPARG gene copy number from TCGA bladder cancer cohort (n= 412 total). **B,** Correlation of PPARG gene expression to *PPARG* absolute copy number (log2). **C,** Heatmap of mRNA

gene expression (RSEM normalized log2) sorted by correlation to PPARG across 412 patients from TCGA bladder cancer cohort.

Supplementary Figure 2.

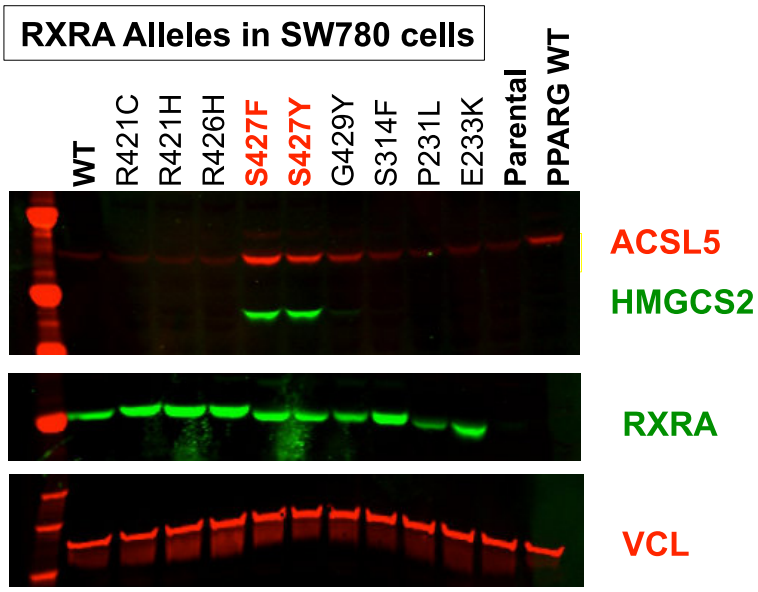

Supplementary Figure 2. PPARG pathway is activated by overexpression of RXRA S427F/S427Y, but not other mutant alleles in bladder cancer cells.
Western immunoblot analysis of lysates from SW780 cells ectopically expressing a variety of RXRA mutant alleles. Comparison of protein expression levels of target genes HMGCS2 and ACSL5 relative to RXRA and loading control VCL, vinculin.

Supplementary Figure 3.

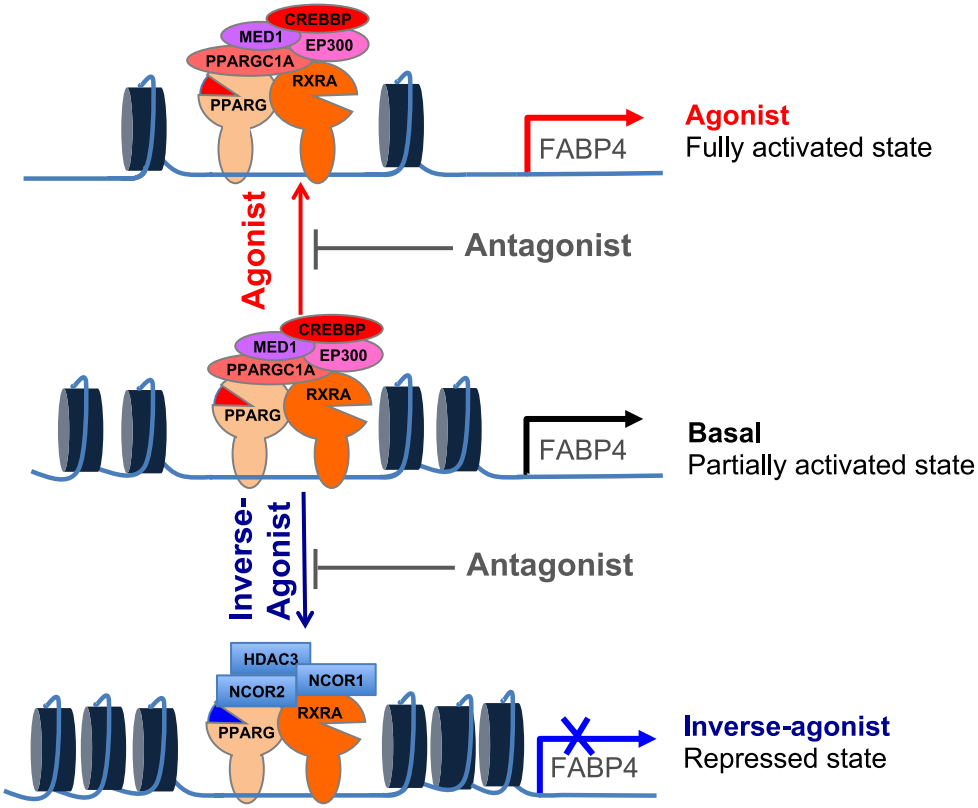

Supplementary Figure 3. Representation of the effects of ligand-dependent modulation on the PPARG interactome. In the basal state for PPARG-activated bladder cancer cells, PPARG is moderately activated (middle). Agonist activation further increases interactions with co-activators, induces histone acetylation, chromatin remodeling, and induces transactivation of target genes by the PPARG complex (top), while inverse-agonists induce interactions with co-repressors, resulting in repression of transactivation through recruitment of corepressors and histone deactylases (bottom). PPARG antagonists block the effects of either agonists or antagonists.

Supplementary Figure 4.

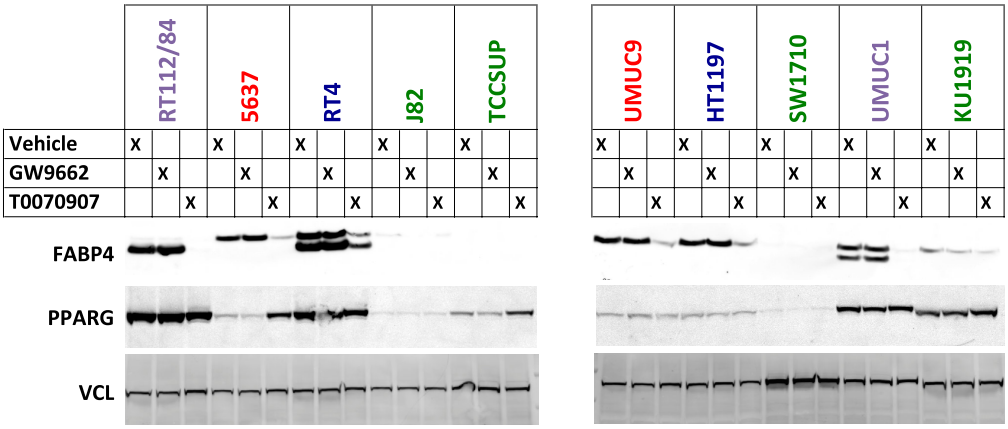

Supplementary Figure 4. Downregulation of FABP4 protein by treatment of PPARG-activated bladder cancer cell lines by inverse-agonist T0070907. Western immunoblot analysis of lysates from bladder cancer cell lines treated for 7 days with vehicle (DMSO), antagonist (GW9662 @ 100nM), and inverse-agonist (T0070907 @ 100nM).

Supplementary Figure 5.

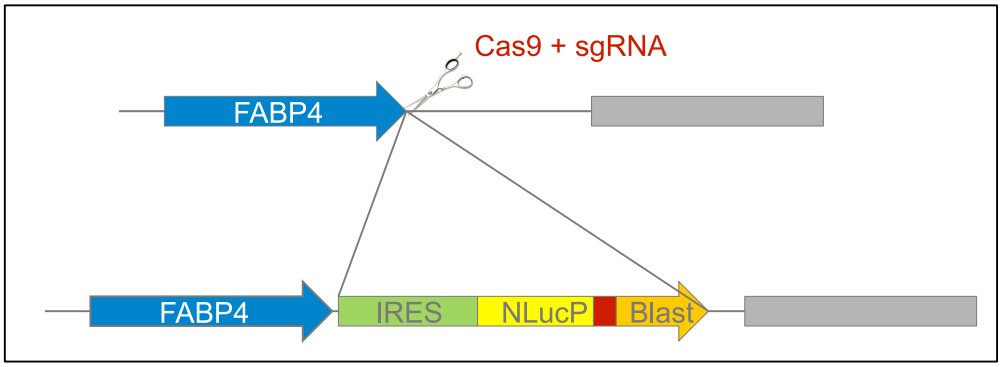

Supplementary Figure 5. Genome engineering scheme for generating reporter cell line. To generate NanoLuc reporter cell line in PPARG-activated RT112/84 cells by inserting NanoLuciferase gene into the 3'UTR of FABP4, a canonical PPARG target gene.

Supplementary Figure 6.

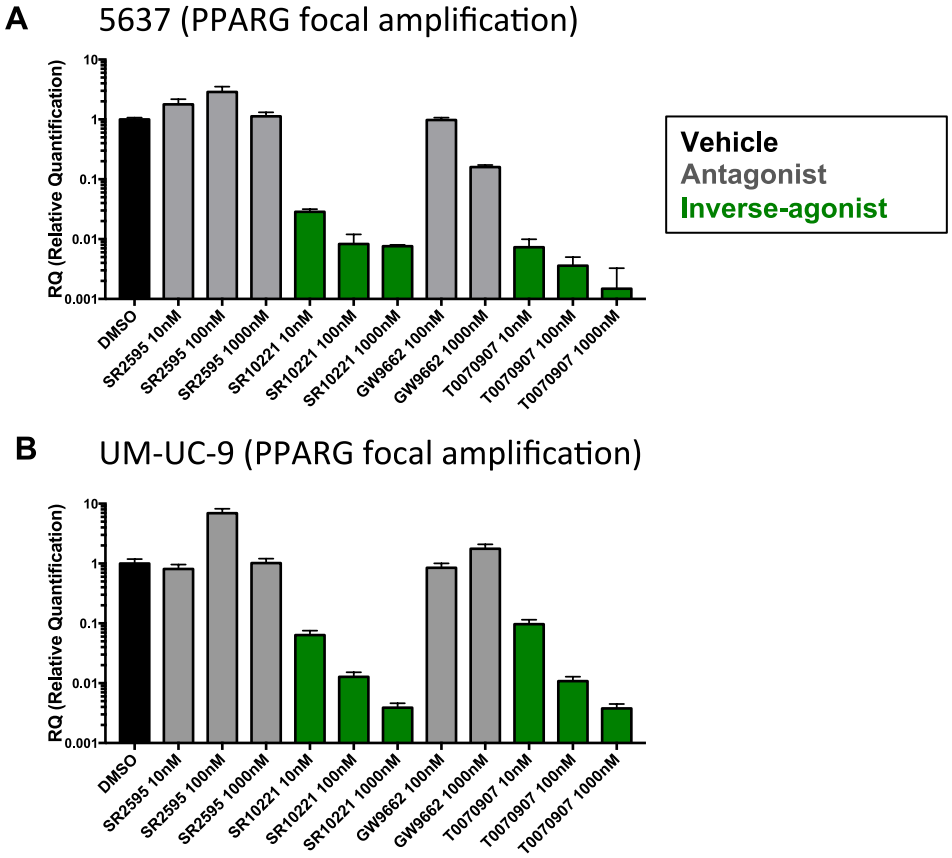

Supplementary Figure 6. Basal expression of FABP4 is reduced by PPARG inverse agonists, but not antagonists. TaqMan qRT-PCR gene expression analysis of FABP4 after overnight treatment with indicated modulators in **A,** 5637 and **B,** UM-UC-9. Data are reported as relative quantification (RQ) for FABP4 compared to GAPDH for test sample after normalization to DMSO control (mean +/- SD, n=3).

Supplementary Figure 7.

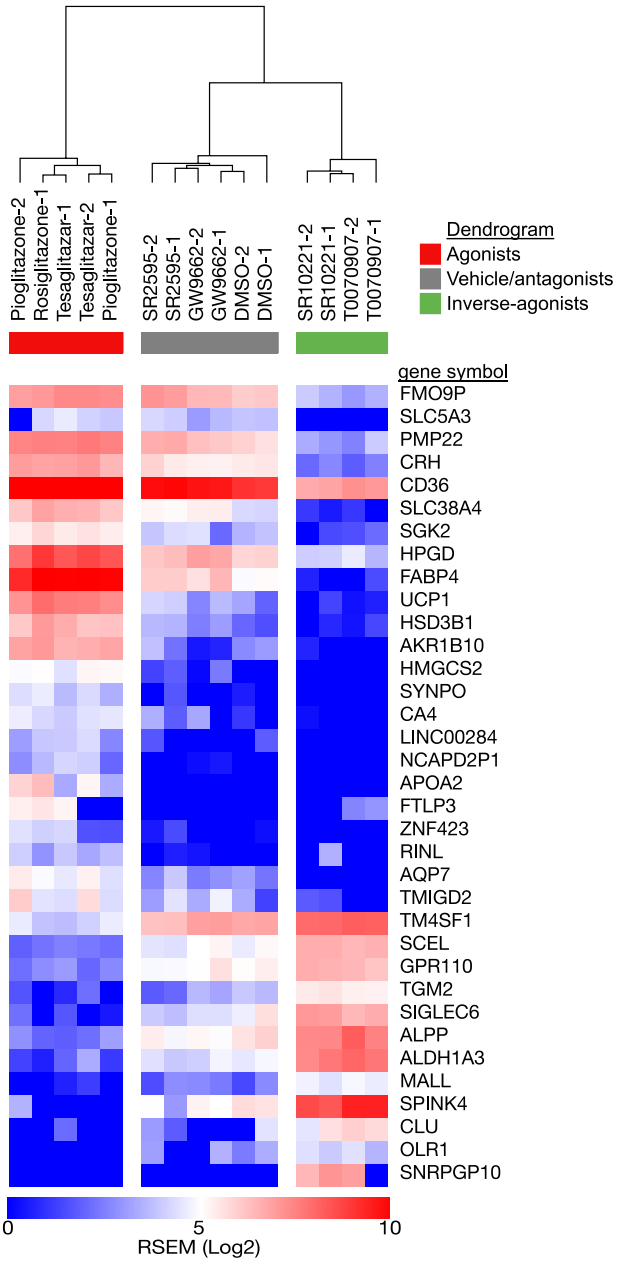

Supplementary Figure 7. Lipid metabolism genes are inhibited by PPARG inverse-agonists. Heat map of some of the top differentially regulated genes in UM-UC-9 cells treated with PPARG modulators for 7 days at 500nM; inverse-agonists (T0070907, SR10221), vehicle, antagonists (GW9662, SR2595), and agonists (Rosiglitazone, Pioglitazone, Tesaglitatzar). RNA sequencing data is reported as transcripts per million (TPM) (log2) with heat map generation and hierarchical clustering of columns performed using Morpheus software package https://software.broadinstitute.org/morpheus/).

Supplementary Figure 8.

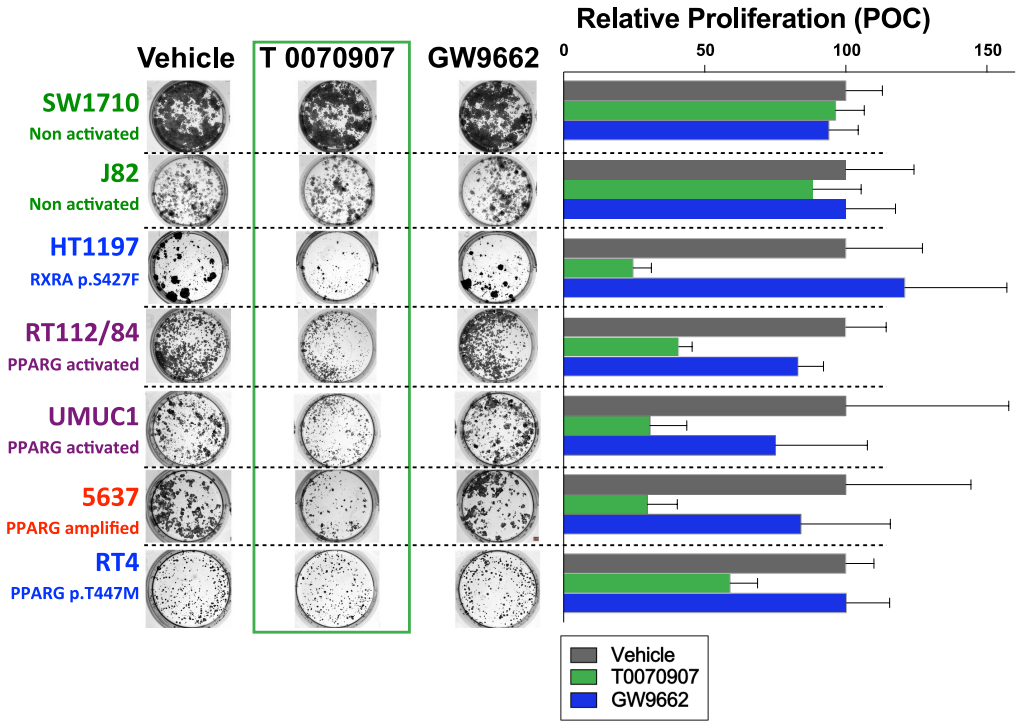

Supplementary Figure 8. PPARG inverse-agonists inhibit proliferation of PPARG activated bladder cancer cell lines in clonogenic assays. Clonogenic growth assays of bladder cancer cell lines after treatment for 7-19 days with PPARG modulators (100nM), as indicated, and DMSO as vehicle control. Clonogenic proliferation at the end of the experiment was evaluated by visualization of colonies by crystal violet staining (left), and quantitatively by UV absorption of crystal violet extracted from samples (right). Data are relative proliferation of test samples compared to vehicle as percent of control. Graph represents mean POC +/- SEM (n=3).

Supplementary Figure 9.

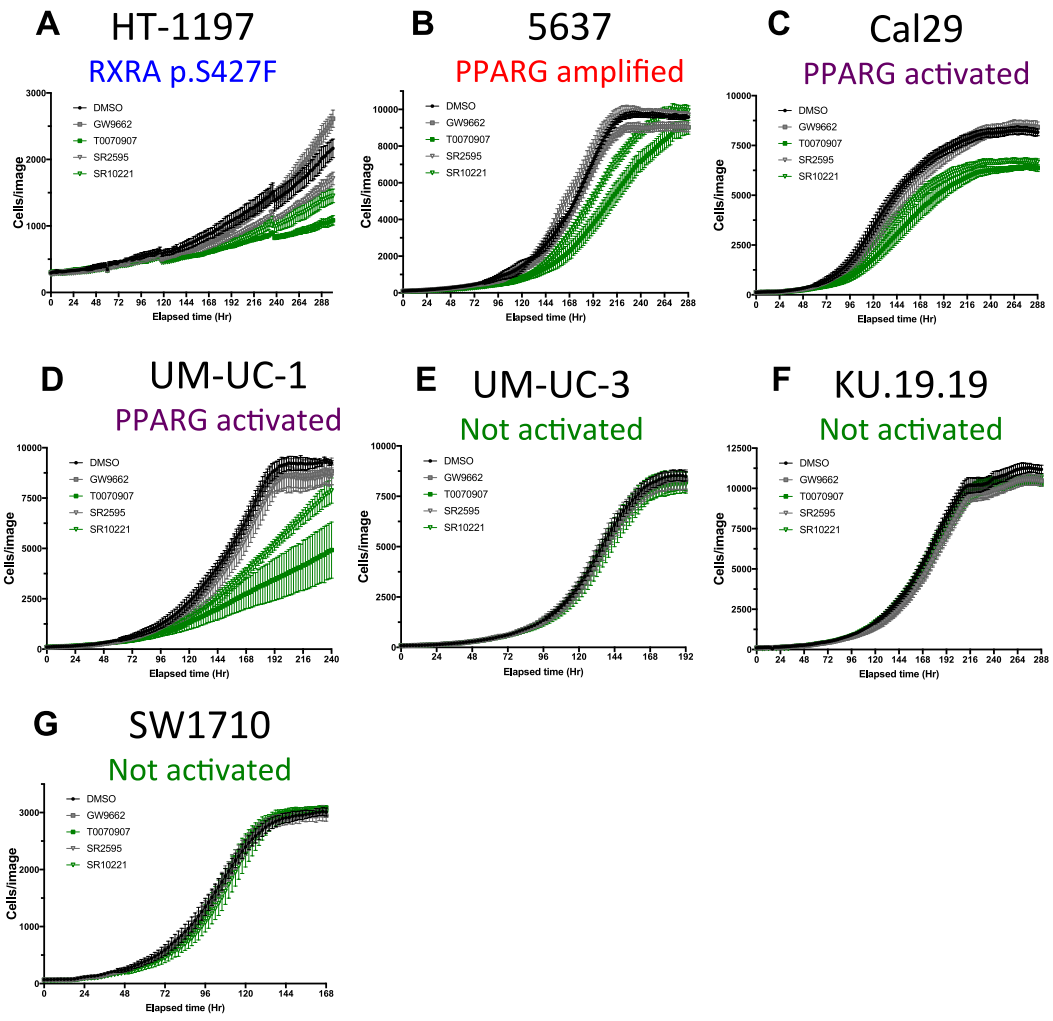

Supplementary Figure 9. PPARG inverse-agonists, but not antagonists, inhibit proliferation of PPARG-activated bladder cancer cell lines. Kinetic proliferation assay measuring the effect of 100nM modulator on growth rate over time in bladder cancer cell lines including **A,** HT-1197 (RXRA p.S427F), **B,** 5637 (*PPARG* amplified) **C**, Cal 29 (PPARG activated), **D,** UM-UC-1 (PPARG activated), **E,** UM-UC-3 (no alteration), **F,** KU19.19 (no alteration), and **G,** SW1710 (no alteration).

Supplementary Figure 10.

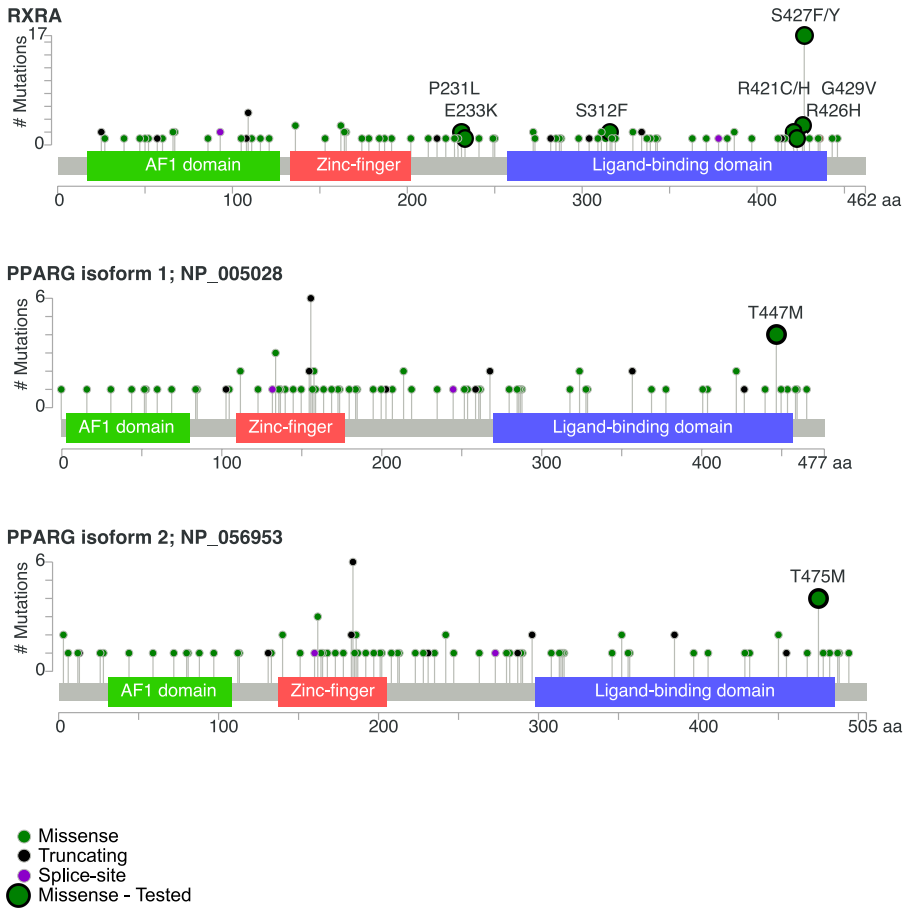

Supplementary Figure 10. Somatic alterations in RXRA and PPARG. Pan-cancer genomics analysis of all non-provisional studies in cBioportal (2,3) accessed on July 19, 2017, displaying mutations in lollipop plot format to indicate the number of samples with each indicated alteration. Multiple isoforms of PPARG result from different translational start sites. PPARG isoform 2, NP_056953, is the more common reference sequence used, however this isoform is preferentially expressed in adipocytes. PPARG isoform 1, NP_005028, is the dominant isoform in other tissues, including bladder. Numbering for both PPARG isoforms is shown. RXRA and PPARG mutant alleles tested within this manuscript are indicated by an enlarged green circle with outline.

Supplementary References:

1. Broad Institute TCGA Genome Data Analysis Center. Analysis-ready standardized TCGA data from Broad GDAC Firehose 2016_01_28 run. https://doi.org/10.7908/C11G0KM9 **2016**.
2. Cerami E, Gao J, Dogrusoz U, Gross BE, Sumer SO, Aksoy BA*, et al.* The cBio Cancer Genomics Portal: An Open Platform for Exploring Multidimensional Cancer Genomics Data: Figure 1. Cancer Discovery **2012**;2:401-4
3. Gao J, Aksoy BA, Dogrusoz U, Dresdner G, Gross B, Sumer SO*, et al.* Integrative Analysis of Complex Cancer Genomics and Clinical Profiles Using the cBioPortal. Science Signaling **2013**;6:pl1-pl